A proof-of-principle study for performing enzyme bioassays using substrates immobilized in a leaky optical waveguide

Gupta, Ruchi

DOI:
10.1016/j.snb.2017.01.053

Document Version
Peer reviewed version

Citation for published version (Harvard):
Gupta, R 2017, 'A proof-of-principle study for performing enzyme bioassays using substrates immobilized in a leaky optical waveguide', Sensors and Actuators B: Chemical, vol. 244, pp. 549-558.
https://doi.org/10.1016/j.snb.2017.01.053

A Proof-of-Principle Study for Performing Enzyme Bioassays Using Substrates Immobilized in a Leaky Optical Waveguide

Corresponding author: Ruchi Gupta, Department of Chemistry, University of Hull, Cottingham Road, Hull, HU6 7RX, UK; Email: ruchi.gupta@hull.ac.uk; Phone: +44 148 246 6552.

Co-authors: Nicholas J. Goddard, Process Instruments (UK) Ltd, March Street, Burnley, BB12 0BT, UK; Email: nick.goddard@processinstruments.net; Phone: +44 128 242 2835.

Abstract

This work is a proof-of-principle study on the feasibility of performing enzyme bioassays using a dye-doped leaky waveguide (DDLW) where the substrate was immobilised in the entire volume of the waveguide and the fraction of light confined in the waveguide interacted with the absorbing product formed as a result of the enzyme's action on the substrate. The immobilisation of the substrate in the waveguide offers the following benefits: (1) The coloured product was still immobilised in the waveguide, and thus unable to diffuse away from the sensing region in the waveguide, which would otherwise lead to a rapid loss of the absorbance signal. (2) The interaction between the optical mode and the immobilised product in the waveguide was maximised, resulting in an experimentally determined sensitivity 57.5 times higher than total internal reflection (TIR). (3) Because of the small volume of the waveguide, a high local concentration of ~1.61 mM could be achieved using a small amount of substrate (7.29 pmol). This is ~100 times lower than the case where the same concentration of the substrate solution is present in a microfluidic flow cell of typical dimensions. (4) The high local concentration of the substrate ensured that the rate of product formation was largely dependent on the concentration of the enzyme in the waveguide. This work demonstrated the suitability of DDLW to perform enzyme bioassays using fluorescein diacetate 5(6)-isothiocyanate and esterase, and the formation of fluorescein was monitored by recording changes in the intensity of the reflected light at the resonance angle. The DDLW has potential applications in drug discovery, clinical diagnostics and industrial biotechnology.

Keywords: Waveguide, immobilised, enzyme, bioassay, absorption.

1. Introduction

Enzyme bioassays are important for drug discovery, clinical diagnostics and industrial biotechnology [1-7]. Enzyme bioassays can be carried out in a number of different ways, but the most common methods are provided in Table 1 [8].

Method	Basic principle	Benefits	Limitations
Initial rate experiments	Measure the rate of initial reaction after mixing enzyme with a large excess of substrate	• Relatively easy to perform • Short timescales	• Requires a sensitive detector to detect low concentrations of the product formed
Progress curve experiments	Measure the time course of enzymatic reaction	• Complete determination of	• Takes relatively long time to perform

		reaction kinetics	
Transient kinetics experiments	Monitor the formation of enzyme-substrate complex	• Provide insights into the enzyme substrate binding	• Instrumentally complex
Relaxation experiments	Enzyme, substrate and product are initially at equilibrium and the reaction is then rapidly perturbed by introducing a change in pressure, temperature or pH	• Understanding of both the forward and backward enzymatic reactions	• Reaction must be reversible

Table 1: Different methods for performing enzyme bioassays including their benefits and limitations

Many different approaches have been used to monitor the appearance of product/ depletion of the substrate with time [9-13], but the most common rely on changes in the optical absorption or fluorescence. Absorption spectrophotometry or fluorimetry in cuvettes or microtitre plates, however, typically require quite large sample volumes, up to 4 ml for a standard 1 cm cuvette or a few hundred µl for a single well of a 96 well microtitre plate. This limitation has been addressed by the use of microfluidic devices, but the detection sensitivity of single pass absorption spectroscopy integrated with microfluidic devices is limited because the optical pathlength is determined by the physical dimensions of microchannels. To improve detection sensitivity while reducing the sample volume techniques such as total internal reflection (TIR) fluorescence or absorbance integrated with microfluidics are used [14-16]. The technique, however, suffers from the disadvantage that the proportion of light in the evanescent field is quite small (typically 0.1-1% of the incident light) requiring high sensitivity detectors to achieve a good signal-to-noise ratio The proportion of light in the evanescent field is higher (20-35% of the incident light) for optical waveguides than TIR, but these are instrumentally complex and require elaborate fabrication methods. For conventional high index waveguides, increasing the proportion of light in the evanescent field means operating closer to cut-off, which requires good control of both the waveguide thickness and refractive index. Higher sensitivity can be achieved if the light in the waveguide rather than in the evanescent field is used to excite fluorescence or perform absorption spectroscopy. This can be achieved with a low index waveguide constructed from a porous transparent material such as a hydrogel where an absorbing or fluorescent species infiltrates into the waveguide and interacts directly with the optical mode in that waveguide. A second advantage of using a low index waveguide is the ease of coupling light in and out of these waveguides using a prism, and is a result of their characteristic partial confinement of light. Low index waveguides have been variously termed Leaky Waveguides (LWs) [8,17-21], Light Condensers (LCs) [22] or Hydrogel Optical Waveguides (HOGs) [23-25], but will be referred to as LWs hereafter.

This work investigates the sensitivity of detection of a LW with a porous waveguide to allow a fluorescent species to infiltrate into the waveguide and hence interact with the optical mode in that waveguide. The theoretical and experimental sensitivity of detection of the porous LW was compared against total internal reflection (TIR). A variant of LW where a dye in present in the waveguide called dye-doped leaky waveguide (DDLW) was subsequently exploited to perform enzyme bioassays by immobilising substrate in the entire

volume of the waveguide and using the interaction between the fraction of light confined in the waveguide and absorbing product formed as a result of the enzyme's action on the substrate. More specifically, the DDLW consisted of an agarose waveguide doped with reactive blue 4 (RB4) on a glass substrate. The immobilised RB4 served two purposes: Firstly, it permits visualisation of the resonance angle as a dip in the reflectivity curve at wavelengths away from the absorption of fluorescein. Secondly, RB4 contains a dichlorotriazine group, which reacts with hydroxy groups in agarose under basic conditions, leaving a reactive monochlorotriazine for subsequent immobilization steps. In this work, the monochlorotriazine group was used to immobilise fluorescein diacetate 5(6)-isothiocyanate (FDAITC) through a diethylenetriamine linker. FDAITC is colourless, but becomes coloured when converted to fluorescein 5(6)-isothiocyanate (FITC) by esterase. Thus, absorption measurements were performed to monitor the formation of the coloured product, FITC, which confirmed the presence of esterase in a sample. Although fluorescence is generally regarded as more sensitive than absorbance, there are two reasons why in this case it is preferable to monitor absorption. Firstly, fluorescence is emitted largely isotropically, meaning that much of the fluorescence is lost. Secondly, in this case it is instrumentally much easier to monitor the light emerging from the prism at a well-defined range of angles. To monitor fluorescence from above would require a transparent flowcell and sample, while monitoring from below would require a truncated prism. In addition, fluorescence is usually excited and detected using relatively expensive instrumentation such as lasers, photomultipliers, cooled charge coupled device (CCD) cameras or electron-multiplying CCD cameras In contrast, the absorbance data in this work was acquired using a low cost white light emitting diode (LED) and a simple and inexpensive complementary metal oxide silicon (CMOS) camera.

2. Experimental

2.1 Chemicals and Materials

1 mm thick glass slides and 1 cm pathlength cuvettes were purchased from VWR (Leicestershire, UK). Ethanol, acetone, phosphate buffered saline (PBS), fluorescein 5(6)-isothiocyanate (FITC), fluorescein diacetae (FDA), esterase, FDA 5(6)-isothiocyanate (FDAITC), reactive blue 4 (RB4, 35%), sodium hydroxide, potassium chloride, sodium carbonate, sodium bicarbonate, diethylenetriamine (99%) and glutaraldehyde were purchased from Sigma-Aldrich (Gillingham, UK). The enzymatic activity of the esterase used was ≥50 U/mg. Ultrapure^{TM} LMP agarose was obtained from Life Technologies (Paisley, UK).

2.2 DDLW device fabrication

Glass squares of ~25.4 mm by 25.4 mm were cleaned in soap solution, de-ionised water and ethanol consecutively for 30 min each using an ultrasonic bath. 2% (w:v) agarose solution was heated in a microwave oven until agarose was fully dissolved. The solution was placed on a hot plate set at 95 °C, 12.5 µl of 25% (v:v) glutaraldehyde was added to 10 ml solution and allowed to react for 15 min. Subsequently, the solution was spin coated at a speed of 2250 rpm for 30 s. As shown in the inset in Figure 1 (b), the plate used to make a flow cell consisted of two inlets and a single outlet, a recessed Y-shaped cavity 0.2 mm deep and a groove to mount an O-ring. The Y-shaped flow channel was 4 mm wide. The plate was fabricated by CNC machining of a 3 mm thick black acrylic sheet. The plate was placed on an agarose coated glass slide and held in place using a fixture clamped on top. To visualise the resonance angle, a freshly prepared RB4 solution containing 0.78 mM of the dye, 0.268 M KCl and 10 mM NaOH was pumped on top of the agarose coated slide for 15 minutes. This resulted in a dip in the reflectivity curve at the resonance angle.

2.3 Instrumentation

As shown in Figure1 (a), an ocean optics spectrometer (USB4000 UV-Vis) in combination with a tungsten-halogen lamp (HL2000), cuvette holder assembly and optical fibres (FC-UV400-1) was used to perform the enzyme bioassay using single pass absorption spectroscopy. A schematic of the instrumentation used to perform the enzyme bioassays using DDLW is shown in Figure 1 (b). Briefly, a BK7 equilateral prism made (Qioptic Photonics, Denbighshire, UK) was used to couple light in and out of the DDLW device. The light source, a white LED (W57L5111P, Roithner Lasertechnik, Vienna, Austria) and camera (Pixelink, Ottowa, Canada) were mounted on rails, which were connected to goniometers to control their angular position. The end of the LED was sawn off and the cut end sanded with 1200 grit emery cloth, then polished successively with 30, 10, 3 and 1 µm diamond lapping film to obtain a flat end of good optical quality. An achromatic doublet was used to obtain a collimated beam. Light was then passed through a cylindrical lens to obtain a wedge-shaped beam with a wedge angle of ~14° in air or ~9° in the prism. The output of the DDLW was passed through a transmission grating and an achromatic doublet to focus it onto the camera. For single wavelength scans, a 491 nm laser (Cobolt Capypso, Cobolt AB, Solna, Sweden) was used as the light source and a 10 mm diameter silicon photodiode (Centronic OSD100-6, RS components, Corby, UK) was used as the detector.

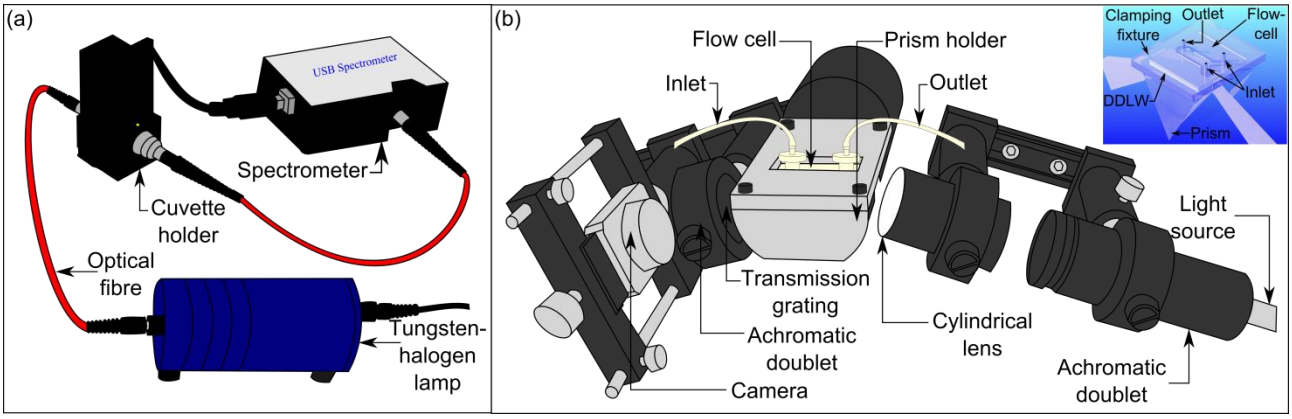

Figure 1: Schematic of the instrumentation for (a) single pass- and (b) DDLW-based broadband absorption spectroscopy (where the inset shows prism, DDLW and flow cell assembly with respect to the incoming and reflected light. The flow cell was black in colour, but is shown to be transparent to illustrate how components stacked on top of each other)

2.4 Methodology

2.4.1 Enzyme bioassay using single pass absorption spectroscopy

Stock solution of 5 mg/ml FDA was prepared in acetone. The lamp was turned off and the dark spectrum (wavelength dependent I_d) was captured. Subsequently, the lamp was turned on and allowed to warm up for at least 30 minutes. A cuvette was filled with 3 ml of PBS and 20 µl of the FDA stock solution. Thus, the concentration of fluorescein diacetate in the cuvette was ~78.9 µM. The cuvette was placed in the path of the light beam consecutively and the corresponding intensity of transmitted light (i.e. I_o) was recorded. The integration time was set to 100 ms and number of scans to average was 10. 2.58 µg ml^{-1} (or 15.4 nM or 0.129 U/ml) of esterase was added to the cuvette, mixed thoroughly and the intensity of transmitted light (i.e.

I) was recorded after every ~1.1 s. The values of I_o, I and I_d were substituted in Beer-Lambert law to obtain time dependent absorbance spectra. Subsequently, the average absorbance value between 493 nm and 497 nm was plotted against time. The above procedure was repeated for 1.31, 0.66, 0.33 and 0.17 µg ml^{-1} of esterase. The same experiment was repeated for a fixed concentration, 2.58 µg ml^{-1}, of esterase, but different concentrations of FDA.

2.4.2 Enzyme bioassay using DDLW

The relationship between camera pixel and wavelength was determined by introducing interference filters of known wavelength in the path of incident light and recording the corresponding pixel position of the reflected light. The relationship between the camera pixel number and wavelength is given by: $N=5994.53-8.95\times\lambda$ (r^2: 0.999) where N is the pixel number and λ the wavelength in nm. The camera integration time was set to 25 ms. A glass slide was placed on top of the prism and an output was captured, which was used to normalise all other images. A dark image was captured with the LED turned off. The DDLW was washed with PBS and 100 mM bicarbonate buffer of pH 9.5. Subsequently, ~1.85 M diethylenetriamine solution prepared in bicarbonate buffer was recirculated on top of the DDLW for 60 min. After a PBS wash, a solution containing ~78.9 µM FDAITC in PBS was allowed to react with the amine groups for 30 min. The device was then washed with PBS. Esterase solution was introduced in the flow cell, the enzyme was allowed to act on the FDAITC for 3 h, and the output of the DDLW was captured at intervals of 30 s. All these fluids were pumped through the flow cell using a peristaltic pump at a flow rate of 0.3 ml min^{-1}. The image analysis was performed using ImageJ. Briefly, the dark image was subtracted from all output images, which were then normalised using a white image recorded at the same integration time but with a glass chip instead of the waveguide, and the value corresponding to the dip position was extracted for all wavelengths. The values obtained for images for DDLW before and after 3 hour treatment with esterase solution were substituted in Beer-Lambert law to obtain the absorption spectrum.

3. Results and discussion

3.1 Single pass absorption spectroscopy

FDA was introduced in enzymatic studies by Guilbault *et. al.* [26] because it is hydrolysed by a number of enzymes including esterases. FDA is now widely used to measure the activity of general esterases in a variety of samples such as soil, lake water and living cells [27-32]. The reaction scheme between FDA and esterase is provided in Figure 2. The activity of esterases is typically measured by quantifying the concentration of coloured fluorescein as the enzyme acts on the colourless FDA. FDA is weakly absorbing because there is no charge delocalisation over the extended π structure of the molecule, whereas the dianionic form of fluorescein absorbs strongly at ~490 nm with a shoulder around 475 nm [33]. FDA hydolyses rapidly at alkaline pH (7.5-9.5), while the activity of esterase is strongest at ~pH 8.0. Thus, as a compromise, the enzyme assay was carried out at pH 7.4.

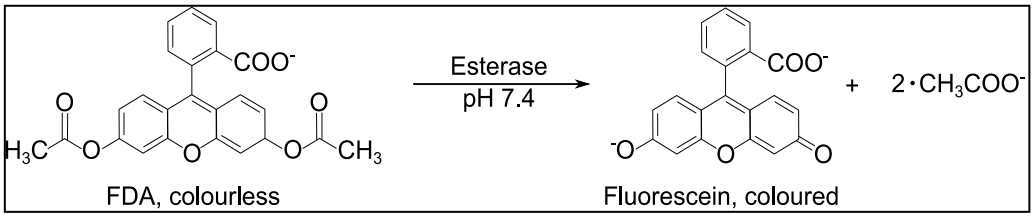

Figure 2: Reaction scheme for the hydrolysis of FDA by esterase

A summary of enzyme bioassays performed using single pass absorption spectroscopy in a cuvette is provided in Figure 3. Figure 3 (a) shows the evolution of absorption spectra as FDA is converted to fluorescein with time interval of 1 min between traces starting ~30 s after adding esterase. As expected, the absorption increases with time after the addition of esterase. For this particular case, the concentration of FDA was 78.9 µM. Figure 3 (b), which is a plot of average absorbance between 493 nm and 497 nm (i.e. 4 nm wide window around the wavelength at which absorbance peak was observed) against time, shows that the initial rate of change of absorbance (i.e. at time=0 in Figure 3 (b), which is within 30 s of adding esterase to the substrate solution) is independent of the enzyme concentration when the substrate concentration is in the range between 19.8 µM and 78.9 µM (i.e. at least ~1260 times higher than esterase concentration). Inset (i) in Figure 3 (c) illustrates that when the substrate concentration is 78.9 µM, the initial rate of change of absorbance is linearly related to the enzyme concentration. The relationship between the two is given by the following equation: $R_t=-1.73\times10^{-4}+2.87\times10^{-3}\times c$($r^2$: 0.999) where c is the enzyme concentration (µg ml^{-1}) and R_t is the initial rate of change of absorbance (s^{-1}). Figure 3 (c) shows that for esterase solutions of concentrations 0.66 µg ml^{-1}, 1.31 µg ml^{-1} and 2.58 µg ml^{-1}, plot of absorbance against time rises exponentially to a maximum value, which implies that the rate of change of absorbance decreases within 500 s (i.e. the duration of the experiment). This is because as the substrate is used up, the enzyme's active sites are no longer saturated and hence substrate concentration becomes rate limiting. In contrast, for esterase solutions of concentrations 0.17 µg ml^{-1} and 0.33 µg ml^{-1}, the exponential time constant for the plot of absorbance against time is so long that the rate of change of absorbance appears to be constant within 500 s. This in turn suggests that at these low concentrations of the enzyme, the amount of substrate used up over the duration of the experiment is insignificant compared to its initial concentration. As a result, the substrate concentration is always high enough to saturate the esterase's active sites.

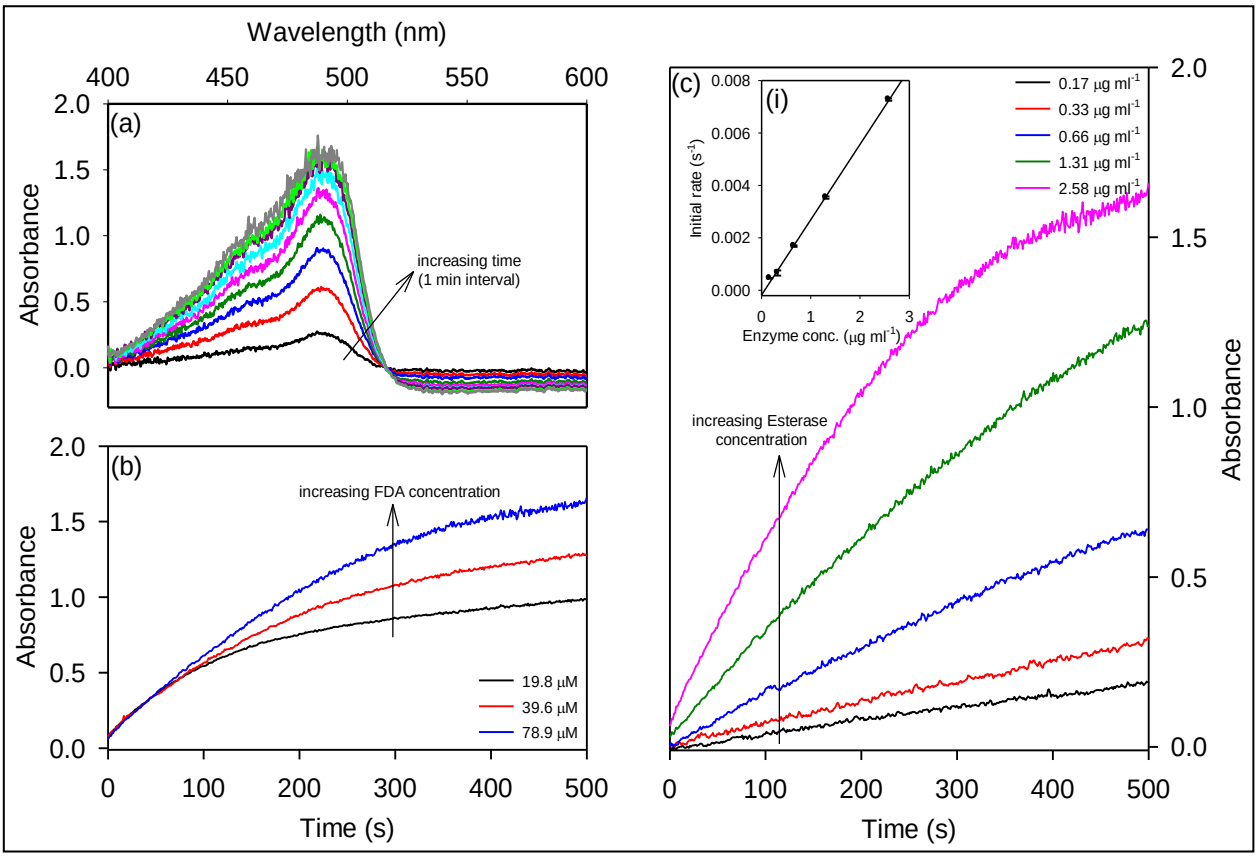

Figure 3: (a) Absorbance spectra as 78.9 μM FDA is converted to fluorescein on adding 2.58 μg ml^{-1} of esterase, time-varying absorbance for (b) 2.58 μg ml^{-1} of esterase but different concentrations of FDA, and (c) 78.9 μM of FDA but different concentrations of esterase (where inset (i) shows the initial rate of change of absorbance *versus* enzyme concentration and error bars are too small to be visible)

3.2 Comparison of DDLW- versus TIR-based absorption

The sensitivity of the DDLW to absorption in the waveguide layer can be determined by first finding the real part of the mode effective index, which then allows the coupling angle to be determined following which the reflectivity at the coupling angle to be calculated. We can determine the modes of a LW by using a simple model that consists of a plane waveguiding layer of thickness h and refractive index n_1 bounded on one side by a semi-infinite (much thicker than the wavelength) substrate of higher refractive index (n_0) than the waveguide layer and on the other side a semi-infinite cover layer of a lower refractive index n_2. Figure 4 shows this structure diagrammatically, with the addition of a coupling prism of index n_0.

The mode equation for this structure can be written as:

$$\Phi_{tot} = 2\Phi_z + \Phi_{10} + \Phi_{12} = 2m\pi \qquad (1)$$

Where Φ_{tot} is the total phase shift for one complete back-and-forth reflection between the two waveguide/substrate boundaries, Φ_z is the phase shift for the propagation of the wave from one boundary to the other, Φ_{10} is the phase shift on reflection at the waveguide/substrate boundary and Φ_{12} is the phase shift on reflection at the waveguide/cover boundary. To satisfy the transverse resonance condition, Φ_{tot} must be an integral multiple of 2π.

From optical theory we obtain:

$$\Phi_Z = \frac{2\pi h}{\lambda}\left(\sqrt{n_1^2 - \beta^2}\right)$$

$$\Phi_{10} = \pi \qquad \text{for TE modes and TM modes where } \theta_i > \theta_p$$
$$= 0 \qquad \text{for TM modes where } \theta_i < \theta_p$$

$$\Phi_{12} = -2\tan^{-1}\left[\frac{n_1^{2p}}{n_2^{2p}}\sqrt{\frac{\beta^2 - n_2^2}{n_1^2 - \beta^2}}\right] \qquad p = 0 \text{ for TE modes, 1 for TM modes}$$

Where β is the real part of the complex effective mode index $N = \beta + iK$. Thus, equation (1) becomes:

$$2m\pi = \frac{4\pi h}{\lambda}\left(\sqrt{n_1^2 - \beta^2}\right) + \pi - 2\tan^{-1}\left[\frac{n_1^{2p}}{n_2^{2p}}\sqrt{\frac{\beta^2 - n_2^2}{n_1^2 - \beta^2}}\right] \tag{2}$$

or,

$$(2m-1)\pi = \frac{4\pi h}{\lambda}\left(\sqrt{n_1^2 - \beta^2}\right) - 2\tan^{-1}\left[\frac{n_1^{2p}}{n_2^{2p}}\sqrt{\frac{\beta^2 - n_2^2}{n_1^2 - \beta^2}}\right] \tag{3}$$

The term Φ_{10} will have the value π in equation (2) because the angle of incidence in the leaky waveguide layer is always greater than the polarisation angle. We can see from these equations that $n_1 > \beta > n_2$, otherwise one of the terms $\sqrt{n_1^2 - \beta^2}$ or $\sqrt{\beta^2 - n_2^2}$ will be imaginary and will not permit real solutions of the equations. This equation cannot be solved analytically so must be solved numerically or graphically to determine β.

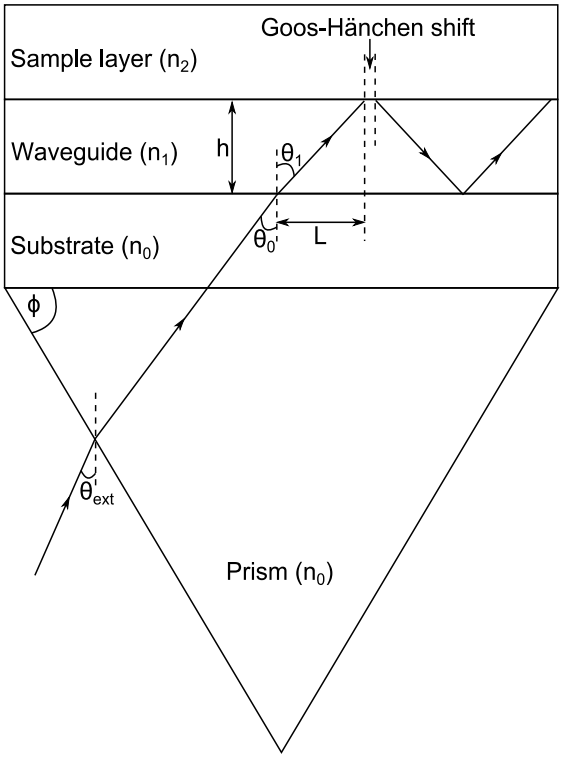

Figure 4: A schematic of the DDLW mounted on a coupling prism

Once we have determined β we can use the transfer matrix method [34] to determine the reflectivity of the structure in the presence of absorption in either the waveguide or cover layer. Firstly we can determine the angles in each layer from:

$$\sin\theta_m = \frac{\beta}{n_m} \qquad \text{and} \qquad \cos\theta_m = \frac{\sqrt{n_m^2 - \beta^2}}{n_m} \tag{4}$$

Where m = 0, 1 or 2 for the substrate, waveguide and cover layers respectively. The reflection coefficients for the substrate/waveguide and waveguide/cover layers can be determined using the Fresnel equations:

$$r_{mn} = \frac{\left(n_n/n_m\right)^p n_m\cos\theta_m - \left(n_m/n_n\right)^p n_n\cos\theta_n}{\left(n_n/n_m\right)^p n_m\cos\theta_m + \left(n_m/n_n\right)^p n_n\cos\theta_n} = \frac{\left(n_n/n_m\right)^p \sqrt{n_m^2-\beta^2} - \left(n_m/n_n\right)^p \sqrt{n_n^2-\beta^2}}{\left(n_n/n_m\right)^p \sqrt{n_m^2-\beta^2} + \left(n_m/n_n\right)^p \sqrt{n_n^2-\beta^2}} \tag{5}$$

Where mn is 01 for the substrate/waveguide interface and 12 for the waveguide/cover interface. The reflection coefficient for the complete structure is then given by:

$$r = \frac{r_{01} + r_{12}e^{2i\delta_1}}{1 + r_{01}r_{12}e^{2i\delta_1}} \tag{6}$$

Where

$$\delta_1 = \frac{2\pi h n_1\cos\theta_1}{\lambda} = \frac{2\pi h\sqrt{n_1^2-\beta^2}}{\lambda} \tag{7}$$

The intensity reflection coefficient can be determined using:

$$R = \left|r^2\right| \tag{8}$$

The imaginary part of the waveguide complex refractive index (K) can be calculated from the wavelength dependent extinction coefficient ε (M^{-1} m^{-1}) and the concentration c (M) of the dye in the waveguide using:

$$K = \frac{230.4\varepsilon c\lambda}{4\pi} \tag{9}$$

In order to compare the detection sensitivity of absorbance of LW and TIR, modelling was performed using the transfer matrix method. A program using this methodology was written in C++. A recursive descent expression evaluator was built in to the program to permit rapid modification of the structure and scan parameters. In addition, a simplex optimisation algorithm [35] was incorporated to allow the program to obtain the best fit structure parameters for a given experimental reflectivity plot. Figure 5 (a) shows theoretical reflectivity plots for a 1.5 µm thick 10% (w/v) agarose waveguide on a BK7 glass substrate and prism at 491 nm for different concentrations of FITC. It can be seen that at an internal angle of 62.23° the reflectivity is most strongly affected by the presence of the dye. This is the angle at which light is coupled most strongly into the waveguide. Figure 5 (b) shows the reflectivity curve at 491 nm for simple TIR with the same concentrations of FITC solutions above the glass substrate. It can be seen that TIR gives much smaller changes in reflectivity. The inset in Figure 5 (b) shows the peak absorbance at 62.23° (the reflectivity minimum) for the LW and 61.5° (close to the critical angle of 61.4679°) for TIR. At these angles, the LW is theoretically about 32 times as sensitive to absorption as TIR. In addition, the slope of the TIR reflectivity curve near the critical angle is very steep, with the result that very small changes in the critical angle caused by refractive index changes in the sample layer will cause large changes in the reflectivity. In the case of the LW, we can find the position of the minimum very easily using either curve fitting or a simple centre of gravity

algorithm and hence find the value of reflectivity at the minimum. Figure 6(a) shows an experimentally determined series of reflectivity curves for an agarose waveguide spin coated from a 2% solution for the same FITC concentrations as in Figure 5(a). In this case, the agarose waveguide was not treated with RB4 before applying the FITC solutions. It can be seen that the experimentally determined reflectivity minimum in Figure 6 (a) for all concentrations of FITC solutions is lower than Figure 5 (a). A possible explanation is that the local concentration of FITC in the waveguide is six to seven times higher than the bulk concentration because of non-covalent interactions between the agarose and FITC. Based on the estimated agarose repeating unit concentration in the waveguide of 80 mM, this would imply a dissociation constant for an FITC-agarose complex of ~12 mM. FITC does not react with agarose at the pH used in this work (pH 7.4). Additionally, the experimentally determined reflectivity minimum saturated at 1000 µM FITC. Figure 6(b) gives the corresponding experimental reflectivity plots for simple TIR, showing that the changes in reflectivity are much smaller than those of the LW. The inset in Figure 6(b) shows the absorbances for LW (at the reflectivity minimum) and for TIR (at 61.5°). The best fit lines (in the linear region from 0 to 300 µM FITC for the LW) give slopes of 1.96×10^{-3} μM^{-1} for LW and 3.41×10^{-5} μM^{-1} for TIR, showing that experimentally determined sensitivity of LW is 57.5 times higher than TIR.

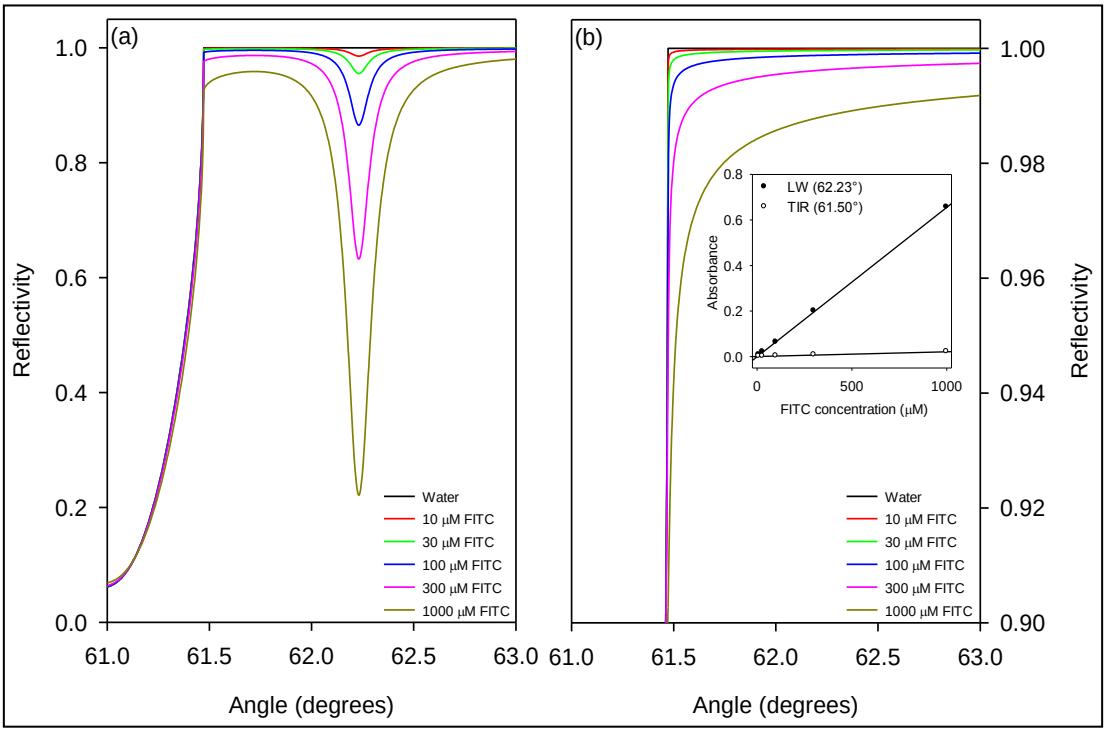

Figure 5: Theoretical plot of reflectivity against angle for a (a) 1.5 µm thick 10% agarose LW (where the concentration of RB4 is zero) and (b) TIR on a BK7 substrate at 491 nm for different concentrations of FITC (where inset compares peak absorbance values *versus* FITC concentration for DDLW and TIR)

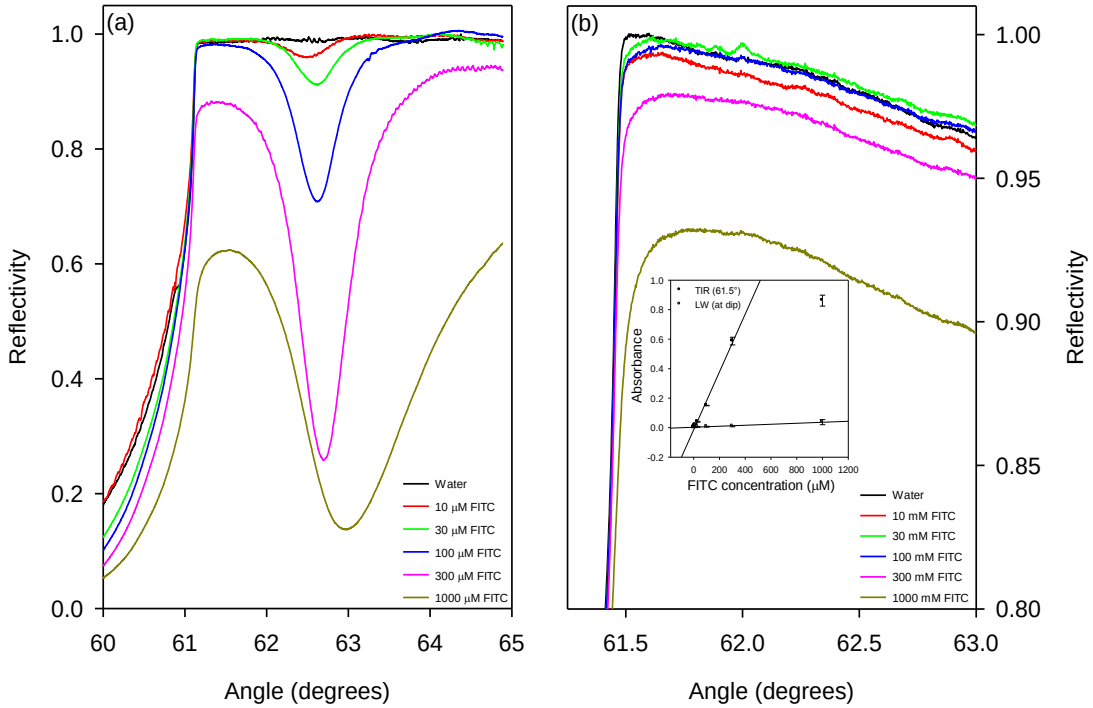

Figure 6: Experimental plot of reflectivity against angle for a (a) LW spin coated from 2% agarose solution and (b) TIR on a BK7 substrate at 491 nm for different concentrations of FITC (where inset compares peak absorbance values *versus* FITC concentration for DDLW and TIR)

3.3 Estimation of the concentration of immobilised substrate

The reaction scheme used for the immobilisation of FDAITC to agarose waveguide is provided in Figure 7. RB4 was first immobilised to agarose waveguide under basic conditions (pH 12) to allow the hydroxy groups in agarose to react with dichlorotriazine group in RB4. In addition, 0.27 M KCl was added to increase the affinity of RB4 to agarose. Subsequently, one of the amine groups in diethylenetriamine was allowed to react with the monochlorotriazine group of RB4 leaving behind a free amine at pH 9.5. These free amine groups reacted with FDAITC. Tests with FITC as a substitute for FDAITC showed that the diethylenetriamine linker increased the amount of FITC immobilised by a factor of ~3 compared to the direct reaction of FITC with RB4 labelled agarose as the maximum absorbance increase by this factor when the linker was used.

Figure 8 (a) shows the experimental and best fit reflectivity curves for the RB4, RB4-FDA before enzymatic hydrolysis and RB4-FDA after 3 h of enzymatic hydrolysis. Taking the reflectivity profile of DDLW consisting of RB4 doped agarose waveguide at 495 nm and fitting using the transfer matrix method gave a waveguide thickness of 1.134 μm, a swelling ratio of 9.75% and an RB4 concentration of 10.87 mM. Based on the swelling ratio, the concentration of agarose in the waveguide was ~20.5% (w:v), which is ~10 times higher than the concentration of agarose solution that was used to fabricate the waveguide. This means that the original gel dried down and when rehydrated, swelled up to 20.5% (w/v) agarose resulting in a thinner, higher refractive index waveguide than the original deposited film. The refractive index of the rehydrated agarose with a swelling ratio of 20.5% is 1.36886 (*versus* 1.34015 for undehydrated gel) at 495 nm. The propagation distance (i.e. the distance for which light travels in the waveguide before it couples out) and penetration depth of the evanescent field for this structure are estimated to be ~14.1 μm and ~0.17 μm respectively. A profile of the optical mode travelling in the agarose of the DDLW structure is provided in Figure 8 (b) and

clearly shows that ~77% of the light is confined in the waveguide, while the remaining 23% is present in the evanescent field. Thus, in case of DDLW, a large proportion of the incident light will interact with the coloured product formed as a result of the enzyme's action on the substrate.

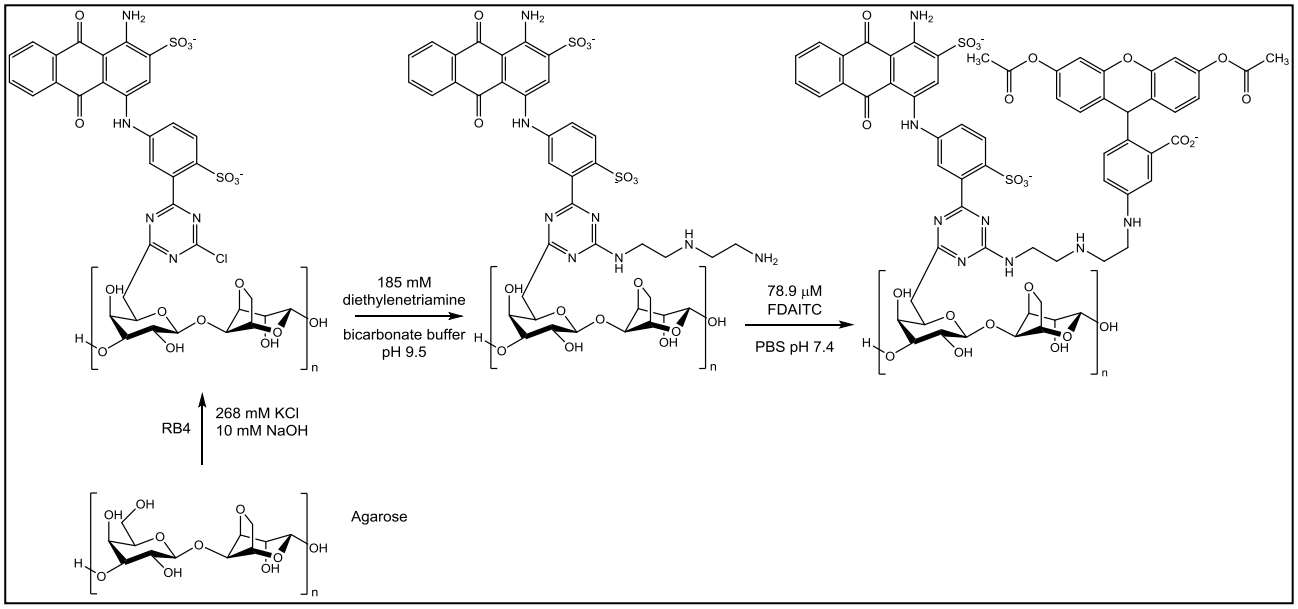

Figure 7: Reaction scheme for immobilising FDAITC to agarose waveguide

After immobilisation of FDAITC, the reflectivity profile was fitted with the addition of an unknown concentration of fluorescein and a real refractive index offset to account for the shift in peak position caused by the refractive index increase following immobilisation. This gave a fluorescein concentration of 383 µM. This implies that ~383 µM of FDAITC in the waveguide was converted to fluorescein because of hydrolysis at pH 7.4 of during the immobilisation process [36]. Esterase (0.24 µg ml^{-1}) was then flowed over the waveguide for 3 h, following which a reflectivity profile at 495 nm was again taken and fitted. This gave a fluorescein concentration of 1.61 mM. Thus, the concentration of FDAITC is estimated to be ~1.61 mM, which is about 20 times higher than the maximum concentration of FDA used in cuvettes for single pass absorption spectroscopy. This in turn implies that while performing the enzyme assay using DDLW, we will be in the regime where the reaction will depend on the concentration of esterase, but will be independent of the concentration of FDAITC. Further, the real refractive index of the waveguide was reduced by 6.11×10^{-4} after the DDLW with FDAITC immobilised in the waveguide was treated with esterase for 3 h. The negative real refractive index shift is thought to be a result of the loss of acetate resulting in a reduction of the molecular mass of the immobilised FDAITC.

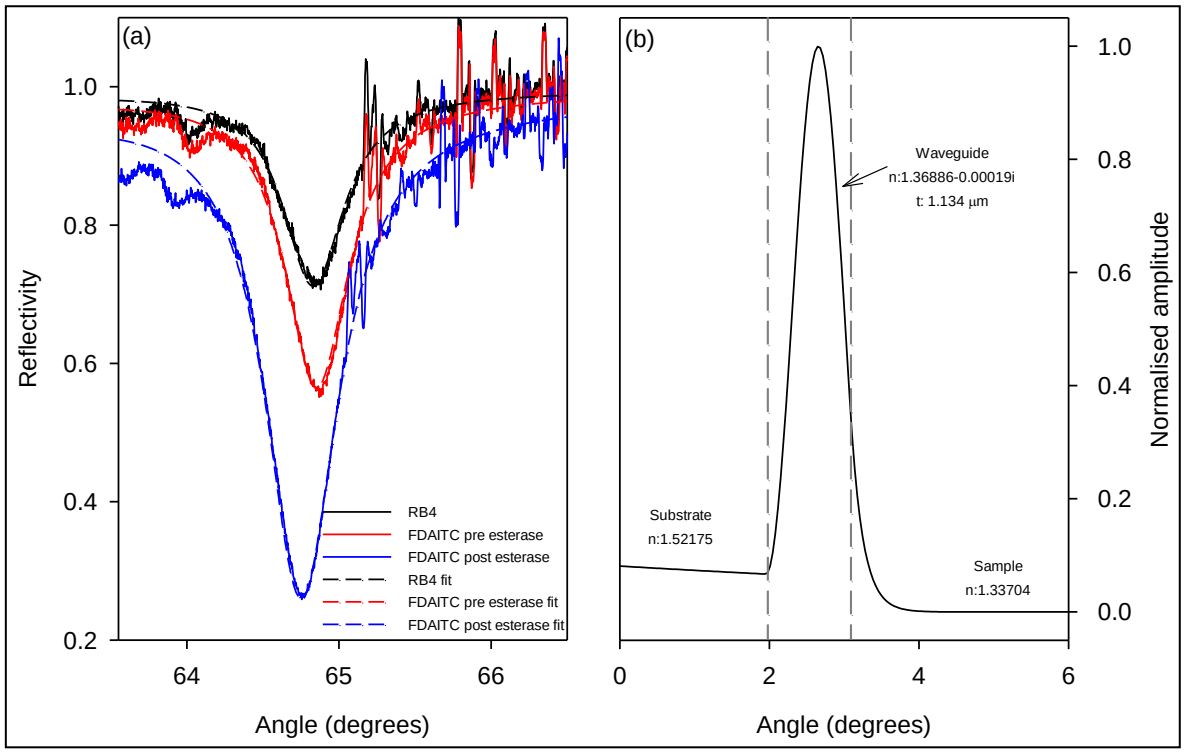

Figure 8: Experimental and best fit reflectivity curves for the RB4, FDAITC before after 3 h of enzymatic hydrolysis, and (b) theoretical profile of the optical mode travelling in the waveguide

3.5 Enzyme bioassay using DDLW

Typical outputs of the DDLW after immobilising FDAITC and irrigating it with 0.24 μg ml^{-1} of esterase in PBS are shown in Figure 9 (a) and (b) respectively. The difference between the two (see Figure 9 (c)) clearly shows the appearance of the band corresponding to the FITC absorption. The difference image was created using the ImageJ image processing program by subtracting the image before esterase from the image after esterase treatment and applying auto contrast enhancement to emphasize the appearance of the absorption band of fluorescein. Only the raw images were used when extracting reflectivity information; no contrast enhancement was applied.

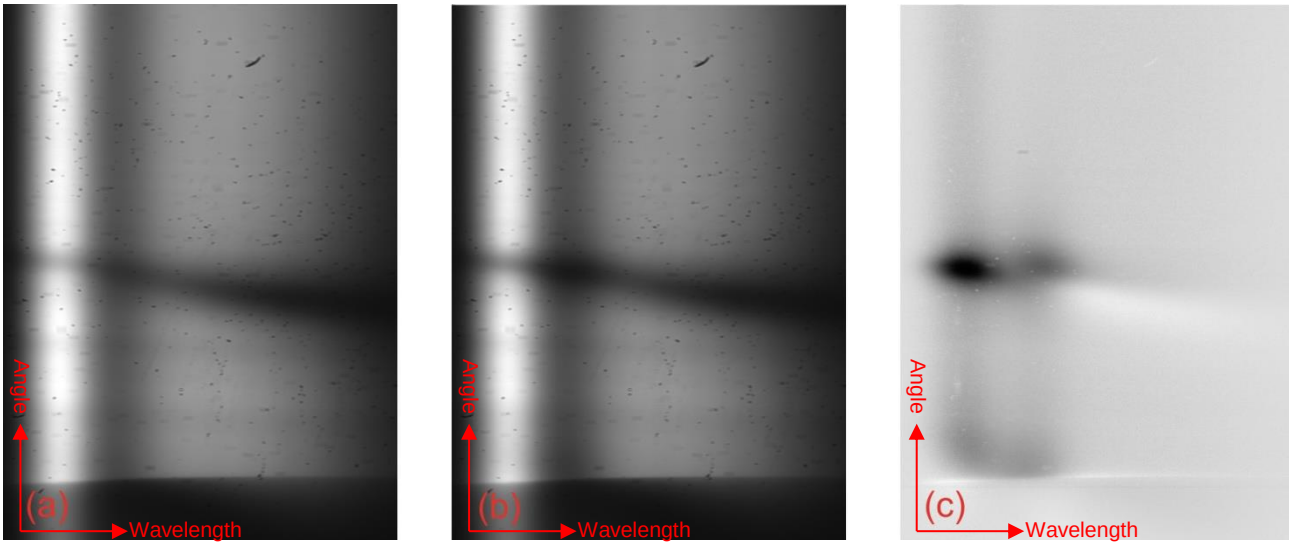

Figure 9: Typical output images of the DDLW (a) after FDATIC immobilisation, (b) esterase treatment and (c) difference between the two after applying auto contrast enhancement

Figure 10 shows the result of irrigating an FDAITC activated device with 0.24 µg ml^{-1} of esterase in PBS. The absorbance has been normalised to aid the comparison with the theoretical plot derived below. As noted in the previous section, the substrate is present in high concentration (at least 1.6 mM) in the waveguide and the enzyme is present in low concentration. Under these conditions, a linear increase in absorbance would be expected, but instead the rate of change of absorbance increases with time. This implies that the enzyme concentration in the waveguide is increasing with time, so the rate of reaction also increases with time. As a first approximation, we assume that the concentration of enzyme at the cover/waveguide interface is constant, that is, there is no depletion of enzyme caused by diffusion into the waveguide. Also, we assume that diffusion of enzyme into the waveguide is sufficiently slow that the concentration of enzyme at the waveguide/substrate interface is much less than the concentration in the cover layer. This puts an upper limit on the range of enzyme diffusion coefficients that will meet this limitation given by:

$$D_{\max} = \frac{h^2}{2t} \tag{10}$$

Under these conditions, we can use a simple linear diffusion model to determine the concentration of enzyme at any point in the waveguide. In this case, we obtain:

$$C = C_0 \operatorname{erfc} \frac{x}{2\sqrt{Dt}} \tag{11}$$

Where C is the enzyme concentration at a distance x from the waveguide/cover interface, C_0 is the enzyme concentration in the cover layer, D is the diffusion coefficient of the enzyme in agarose and t is time. To obtain the rate of reaction, we must integrate equation 11 from 0 (the top of the waveguide) to the height of the waveguide h to obtain the total amount of enzyme that has diffused into the waveguide:

$$\int_0^h C_0 \operatorname{erfc}\left(\frac{x}{2\sqrt{Dt}}\right) dx = C_0 \left[x.\operatorname{erfc}\left(\frac{x}{2\sqrt{Dt}}\right) - \frac{2\sqrt{Dt}}{\sqrt{\pi}} e^{-\frac{x^2}{4Dt}} \right]_0^h = C_0 \left[h.\operatorname{erfc}\left(\frac{h}{2\sqrt{Dt}}\right) - \frac{2\sqrt{Dt}}{\sqrt{\pi}} \left(1 + e^{-\frac{h^2}{4Dt}}\right) \right] \tag{12}$$

The concentration of product will be the integral of equation 12 with respect to time multiplied by the appropriate rate constant k:

$$kC_0 \int_0^T \left[h.\operatorname{erfc}\left(\frac{h}{2\sqrt{Dt}}\right) - \frac{2\sqrt{Dt}}{\sqrt{\pi}} \left(1 + e^{-\frac{h^2}{4Dt}}\right) \right] dt \tag{13}$$

Unfortunately this function cannot be integrated analytically, so must be integrated numerically.

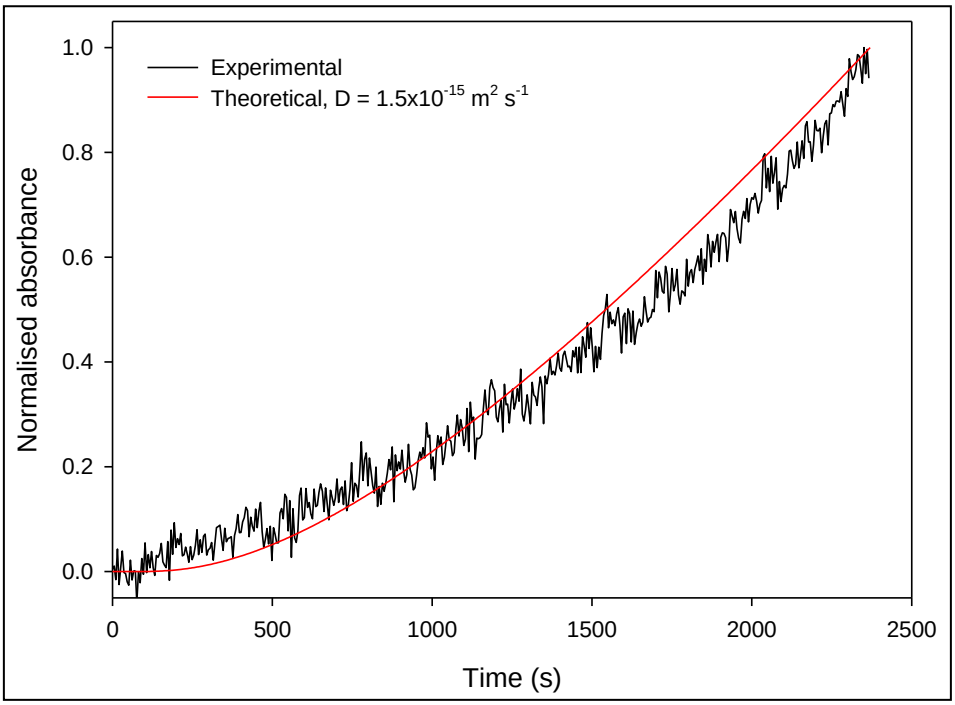

Figure 10: Plot of normalised absorbance against time for an FDAITC chip irrigated with 0.24 µg ml^{-1} esterase in PBS (black trace) and a theoretical plot of normalised absorbance derived from equation 12 for an enzyme diffusion coefficient in agarose of 1.5×10^{-15} m^2 s^{-1}.

Figure 10 shows a theoretical plot based on a diffusion coefficient of esterase in agarose of 1.5×10^{-15} m^2 s^{-1}. This compares with a literature value of ~4×10^{-11} m^2 s^{-1} [37], showing that the waveguide layer significantly hinders the diffusion of enzyme and hence the pore size distribution in agarose waveguides is considerably smaller than esterase. This is because the dehydration/rehydration dramatically reduces the pore size of agarose and is in accordance with the modelling results that indicated that rehydrated agarose waveguides are structurally as well as optically denser than those that have never been dehydrated. Based on the width of light beam, waveguide thickness and width of the microchannel, the substrate volume being sensed was ~4.53 nL. This when multiplied with the estimated concentration of the substrate in the waveguide resulted in ~7.29 pmol of the substrate.

4. Conclusions

A dye-doped leaky waveguide (DDLW) for carrying out enzymatic bioassays has been developed. The DDLW consisted of a substrate, fluorescein diacetate 5(6)-isothiocyanate (FDAITC), immobilised to the agarose waveguide. The reaction of esterase solution on the substrate resulted in the formation of fluorescein tethered to the waveguide. The formation of the absorbing species, fluorescein, was monitored by recording the changes in the intensity of the reflected light at the resonance angle. A mathematical model governing the reflection coefficient at the resonance angle of DDLW was developed and implemented in C++ using a transfer matrix method. The experiments showed that the sensitivity of DDLW to absorbance was 57.5 times higher than TIR. Additionally, as the coloured product formed as a result of the action of the enzyme on the substrate was still immobilised in the waveguide, it could not diffuse away from the sensing region in the waveguide, thereby preventing a rapid loss of the absorbance signal. The immobilisation of the substrate in the small volume of the waveguide resulted in high local concentration of 1.61 mM, while

requiring only 7.29 pmol of the substrate. The high local concentration of the substrate ensured that the rate of product formation was largely dependent on the concentration of the enzyme, which was limited by the rate of diffusion of the enzyme in the waveguide. The future work will focus on devising DDLW with highly porous waveguides and subsequently using them to perform bioassays at different enzyme concentrations.

References

[1] H. Ma, S. Deacon, K. Horiuchi, **The challenge of selecting protein kinase assays for lead discovery optimization**, Expert Opinion on Drug Discovery, 3, (2008), 607-621.

[2] S. Andreescu, J.L. Marty, **Twenty years research in cholinesterase biosensors: From basic research to practical applications**, Biomolecular Engineering, 23, (2006), 1-15.

[3] L. Srigiriraju, P.J. Semtner, T.D. Anderson, J.R. Bloomquist, **Esterase-based Resistance in the Tobacco Adapted Form of the Green Peach Aphid, Myzus persicae (Sulzer) (Hemiptera: Aphididae) in the Eastern United States**, Archives of Insect Biochemistry and Physiology, 72, (2009), 105-123.

[4] C.L. Crespi, V.P. Miller, B.W. Penman, **Microtiter plate assays for inhibition of human, drug-metabolizing cytochromes P450**, Analytical Biochemistry, 248, (1997), 188-190.

[5] R.L. Walsky, R.S. Obach, **Validated assays for human cytochrome P450 activities**, Drug Metabolism and Disposition, 32, (2004), 647-660.

[6] Y.H.P. Zhang, J. Hong, X. Ye, in J.R. Mielenz (Editor), Biofuels: Methods and Protocols, 2009, p. 213-231.

[7] Y.H.P. Zhang, M.E. Himmel, J.R. Mielenz, **Outlook for cellulase improvement: Screening and selection strategies**, Biotechnology Advances, 24, (2006), 452-481.

[8] S. Schnell, M.J. Chappell, N.D. Evans, M.R. Roussel, **The mechanism distinguishability problem in biochemical kinetics: The single-enzyme, single-substrate reaction as a case study**, Comptes Rendus Biologies, 329, (2006), 51-61.

[9] M. Zhang, S. Karra, W. Gorski, **Rapid Electrochemical Enzyme Assay with Enzyme-Free Calibration**, Analytical Chemistry, 85, (2013), 6026-6032.

[10] Y. Li, L. Syed, J. Liu, D.H. Hua, J. Li, **Label-free electrochemical impedance detection of kinase and phosphatase activities using carbon nanofiber nanoelectrode arrays**, Analytica Chimica Acta, 744, (2012), 45-53.

[11] D.O. Lambeth, W.W. Muhonen, **High Performance Liquid Chromatohraphy-based Assays of Enzyme Activities**, Journal of Chromatography B-Analytical Technologies in the Biomedical and Life Sciences, 656, (1994), 143-157.

[12] J.P. Goddard, J.L. Reymond, **Enzyme assays for high-throughput screening**, Current Opinion in Biotechnology, 15, (2004), 314-322.

[13] C.J. Gray, M.J. Weissenborn, C.E. Eyers, S.L. Flitsch, **Enzymatic reactions on immobilised substrates**, Chemical Society Reviews, 42, (2013), 6378-6405.

[14] F. Ma, M. Liu, Z.-y. Wang, C.-y. Zhang, **Multiplex detection of histone-modifying enzymes by total internal reflection fluorescence-based single-molecule detection**, Chemical Communications, 52, (2016), 1218-1221.

[15] M. Tokunaga, K. Kitamura, K. Saito, A.H. Iwane, T. Yanagida, **Single molecule imaging of fluorophores and enzymatic reactions achieved by objective-type total internal reflection**

fluorescence microscopy, Biochemical and Biophysical Research Communications, 235, (1997), 47-53.

[16] P. Siuti, S.T. Retterer, C.-K. Choi, M.J. Doktycz, **Enzyme Reactions in Nanoporous, Picoliter Volume Containers**, Analytical Chemistry, 84, (2012), 1092-1097.

[17] R. Gupta, B. Bastani, N.J. Goddard, B. Grieve, **Absorption spectroscopy in microfluidic flow cells using a metal clad leaky waveguide device with a porous gel waveguide layer**, Analyst, 138, (2013), 307-314.

[18] C. Maims, J. Hulme, P.R. Fielden, N.J. Goddard, **Grating coupled leaky waveguide micro channel sensor chips for optical analysis**, Sensors and Actuators B-Chemical, 77, (2001), 671-678.

[19] M. Zourob, N.J. Goddard, **Metal clad leaky waveguides for chemical and biosensing applications**, Biosensors & Bioelectronics, 20, (2005), 1718-1727.

[20] M. Zourob, S. Mohr, B.J.T. Brown, P.R. Fielden, M.B. McDonnell, N.J. Goddard, **An integrated metal clad leaky waveguide sensor for detection of bacteria**, Analytical Chemistry, 77, (2005), 232-242.

[21] M. Zourob, S. Mohr, P.R. Fielden, N.J. Goddard, **Small-volume refractive index and fluorescence sensor for micro total analytical system (mu-TAS) applications**, Sensors and Actuators B-Chemical, 94, (2003), 304-312.

[22] N.J. Harrick, Internal Reflection Spectroscopy, John Wiley & Sons Inc, New York, 1967.

[23] A. Jain, A.H.J. Yang, D. Erickson, **Gel-based optical waveguides with live cell encapsulation and integrated microfluidics**, Optics Letters, 37, (2012), 1472-1474.

[24] Y. Wang, C.-J. Huang, U. Jonas, T. Wei, J. Dostalek, W. Knoll, **Biosensor based on hydrogel optical waveguide spectroscopy**, Biosensors & Bioelectronics, 25, (2010), 1663-1668.

[25] Q. Zhang, Y. Wang, A. Mateescu, K. Sergelen, A. Kibrom, U. Jonas, T. Wei, J. Dostalek, **Biosensor based on hydrogel optical waveguide spectroscopy for the detection of 17 beta-estradiol**, Talanta, 104, (2013), 149-154.

[26] G.G. Guilbault, D.N. Kramer, **Fluorometric Determination of Lipase, Acylase, Alpha-, and Gamma-Chymotrypsin and Inhibitors of these Enzymes**, Analytical Chemistry, 36, (1964), 409-412.

[27] V.S. Green, D.E. Stott, M. Diack, **Assay for fluorescein diacetate hydrolytic activity: Optimization for soil samples**, Soil Biology & Biochemistry, 38, (2006), 693-701.

[28] T.J. Battin, **Assessment of fluorescein diacetate hydrolysis as a measure of total esterase activity in natural stream sediment biofilms**, Science of the Total Environment, 198, (1997), 51-60.

[29] T.H. Chrzanowski, R.D. Crotty, J.G. Hubbard, R.P. Welch, **Applicability of the Fluorescein Diacetate Method of Detecting Active Bacteria in Fresh Water**, Microbial Ecology, 10, (1984), 179-185.

[30] J.T. Kvach, J.R. Veras, **A Fluorescent Staining Procedure for Determining the Viability of Mycobacterial Cells**, International Journal of Leprosy and Other Mycobacterial Diseases, 50, (1982), 183-192.

[31] N. Steward, R. Martin, J.M. Engasser, J.L. Goergen, **A new methodology for plant cell viability assessment using intracellular esterase activity**, Plant Cell Reports, 19, (1999), 171-176.

[32] J. Szollosi, P. Kertai, B. Somogyi, S. Damjanovich, **Characterisation of Living Normal and Leukemic Mouse Lymphocytes by Fluorescein Diacetate**, Journal of Histochemistry & Cytochemistry, 29, (1981), 503-510.

[33] R. Sjoback, J. Nygren, M. Kubista, **Absorption and Fluorescence Properties of Fluorescein**, Spectrochimica Acta Part a-Molecular and Biomolecular Spectroscopy, 51, (1995), L7-L21.

[34] J. Chilwell, I. Hodgkinson, **Thin-films Field-transfer Matrix Theory of Planar Multilayer Waveguides and Reflection from Prism-loaded Waveguide**, Journal of the Optical Society of America a-Optics Image Science and Vision, 1, (1984), 742-753.

[35] J.A.N.a.R. Mead, **A simplex method for function minimization**, The Computer Journal, 7, (1965), 6.

[36] R.J. Chrost, A. Gajewski, W. Siuda, **Fluorescein-diacetate (FDA) assay for determining microbial esterase activity in lake water**, Ergebnisse der Limnologie, 0, (1999), 167-183.

[37] W. Junge, K. Krisch, H. Hollandt, **Further Investigations on the Subunit Structure of Microsomal Carboxylesterases from Pig and Ox Livers**, European Journal of Biochemistry, 43, (1974), 379-389.